



Surface Morphology of Polymers Examined by Atomic Force Microscopy

Péricles Lopes Santana*, José Roberto R Bortoleto, Nilson Cristina da Cruz, Elidiane Cipriano Rangel and Steven F Durrant

Universidade Estadual Paulista – UNESP Laboratorio de Plasmas Tecnologicos, Sorocaba, SP, Brasil

*Corresponding Author: Péricles Lopes Santana, Universidade Estadual Paulista – UNESP Laboratorio de Plasmas Tecnologicos, Sorocaba, SP, Brasil.

Received: September 09, 2022

Published: November 07, 2022

© All rights are reserved by Péricles Lopes Santana, et al.

Graphical Abstract (GA)



Figure a

Abstract

In this article we introduce some studies of surface morphology in polyolefins, including commercial polymers. Atomic Force Microscopy (AFM) was used to examine the surface roughness of the pristine and plasma-treated samples. A polymer surface in a plasma is exposed to a broad spectrum of ions, electrons and radicals, which cause sputtering and etching and, consequently, increases surface roughness and induce changes in surface chemistry. Today, AFM, is one of the foremost tools for imaging, measuring and manipulating the surface of materials at the nanoscale, being useful in diverse areas such as materials and life science and in engineering, revealing surface roughness, R_{rms} above 1 nm and below 100 nm for the polymers examined by an Atomic Force Microscope at non contact mode..

Keywords: Polymers; Surface Morphology; AFM

Introduction

Solid surfaces present a constant surface area [1], which exhibits a roughness that depends on the size of the observed system [2]. Roughness is related to variations in height over an area produced during fabrication or subsequent accumulation or detachment of particles [3]. The study of surface properties of polymers, pristine or modified by different processes and agents, is impor-

tant not only for understanding of the basic processes taking place during the modification but also for subsequent use of the modified polymers. The modifications may influence the process of polymer coating with metals, adhesion of the deposited metal films (electronic engineering) [4], grafting of the polymer surface with different chemical agents and adhesion and proliferation of living cells (important, for example, for polymer use in tissue engineering)

[5]. Hence, plasma treatments have been used to modify many surface properties of polymeric materials for specific applications [6].

Plasma species are able to induce physical and chemical surface changes in polymers through etching, polymerization and cross-linking), maintaining their bulk properties [6]. Plasma treatment of polymers leads to the creation of new chemical groups [7,8], branching and cross-linking of macromolecules [9] and formation of low molecular weight oxidized structures [10]. The production of new oxidized structures on polymer chains changes the surface morphology and roughness, thus modifying polymer wettability as characterized by surface contact angle [11,12]. The rates of these processes depend on the plasma reactivity. Owing to ablation [13] the surface morphology of polymer is affected too [14]. Surface properties of the plasma modified polymers depend on the exposure time and the gases composition under which the modified specimens are stored [15]. It is known that the aging of plasma-modified specimens results in a pronounced decrease of their surface wettability in argon plasma [13]. Experiments reported in the literature aimed at increasing the wettability of poly(ethylene terephthalate) (PET) fabrics using air plasma treatment have achieved permanent surface modifications that are correlated with both a modified chemical composition caused by air plasma oxidation of the surface and by physical changes in the surface morphology [16].

Plasma treatment has several advantages: only a thin surface layer (from some nm to tens of μm thick) of polymer is modified and the bulk properties are retained, as well as the macro dimensions of the piece; resulting properties of the modified surface layer can be controlled by composition of the ambient atmosphere; good homogeneity of modified surface can be achieved. Control of the process is possible via adjustment of the plasma discharge parameters, gas flows, substrate temperature, discharge power and frequency. The modifications are caused mainly by the interaction of radicals and ions with the polymer surface [17].

Polymer film formation and surface morphology of polymers in general are affected by various parameters including, temperature [18] and synthesis method [19]. High temperatures can produce the diffusion of oxidized degradation species into the bulk and orientation of polar toward the bulk may occur [20]. Surface hydrophilicity is connected with a rearrangement of degradation species on the surface of modified surface [21].

On polymers with cross-linked structures on the top layers, processes of rearrangement may be reduced [22]. Aging effects depend on the creation of an energetically favorable state (thermodynamic equilibrium), then, contaminants from the atmosphere may be adsorbed in order to reduce its surface energy [23]. This suggests that morphological changes may occur.

In general, polyolefins are cheap and easy to process. Polyethylenes, i.e., do not exhibit, printability, hydrophilicity and adhesion of micro-organisms, underscore the need for tailoring the surface [24].

A polymer surface in a plasma is exposed to a large spectrum reactive radicals. Ultraviolet radiation causes etching and consequently increases surface roughness and induces changes in surface chemistry. Indeed, interesting regular surface morphologies after plasma treatment have recently been reported for polymer substrates [25].

One plasma-based mechanism is etching, which involves the impact of the gas plasma species on the polymer surface to control the surface roughness for better wettability, although deliberately nano-structured surfaces tend to be more hydrophobic. It is possible to quantify the extent of the etching caused by the plasma treatment by simple weight loss analysis, in which, depends on the polymer structure and the reactivity of the plasma composition [26].

In semicrystalline polymers, a roughness pattern was observed on cellulose after plasma surface treatment [27], exhibiting micro-sized aligned walls [28], nanosized bumps [29], and fibrils after oxidative plasma treatment on PET films [30]. Nanotextures have also been observed in amorphous polymers, i.e. on polystyrene (PS) films using fluorine/oxygen plasma [31], and after argon/oxygen plasma treatment of PMMA, $(\text{C}_5\text{O}_2\text{H}_8)_n$, films [32], and also reported in Polypropylene, $(\text{C}_3\text{H}_6)_n$ [33].

In Polydimethyl-Siloxane, $(\text{CH}_3)_3\text{SiO}$, quasi-periodic structures were created after fluorine plasma treatment [34], with high surface area nanostructures after oxygen plasma treatment [35], and nanohairs after sulfur hexafluoride plasma treatment [36]. Fibrils with dimensions ranging from 50 to 500 nm and lengths up to 5 μm were also reported after plasma treatment of spin-coated films of different materials [37] PolyMethylMetaAcrylate, PMMA, $(\text{C}_5\text{O}_2\text{H}_8)_n$; Polystyrene, PS, $\text{C}_6\text{H}_5\text{C}_2\text{H}_3$; Polyvinylidene fluoride, PVDF, $-(\text{C}_2\text{H}_2\text{F}_2)$

_n-; Poly(3,4-ethylenedioxythiophene), PEDOT, $(C_6H_6O_2S)_n$; Polypyrrole, PPy, $H(C_4H_2NH)_nH$; and SU-8 photoresist epoxy), being possible to result in antireflecting [32], and cell-adhesive [38] properties and hydrophobicity [29,31,33,34,39].

Many researches have been inspired by superhydrophobic or superhydrophilic surfaces found in natural polymers that exhibit micro and nano-roughness. This roughness not only makes the natural surfaces superhydrophilic ($\theta < 10^\circ$) but also absorbs a lot of water through capillarity. For instance, peat moss has a sponge-like surface structure, which makes it superhydrophilic and helps it absorb water up to about 20 times of its own dry weight [40]. The reverse of superhydrophilicity is superhydrophobicity, which is also greatly influenced by the surface roughness. One of the most common examples of a natural superhydrophobic surface is the lotus leaf, which has micro-roughness covered with nanoscale hydrophobic wax crystals, and this forms a hierarchical structure [41]. Owing to this structure, the lotus leaf has very high water contact angle, $\theta \sim 160^\circ$ and very low water sliding angle $\sigma < 5^\circ$ [42]. The low water sliding angle leads to self cleaning, because water droplets roll over the surface very easily [43]. The water sliding angle depends on θ and the roughness, R [44]. Different techniques have been used to reduce the water sliding angle by manipulating the surface roughness, and in all cases, including polymers, there is a dependence of wettability on surface morphology.

In general, oxidative plasma treatment of polymer surfaces increases R [44]. Surface roughness can be defined from its parameters of surface morphology, such: average or by root mean square height [45]. Measured (effective) roughness. To learn more about the morphology of plasma modified materials which in turn influences the value of the specific surface area, AFM is an outstanding technique. Some data concerning surface structures of polymers using AFM are as follows: PVC, 4.38 nm, PET 1.7 nm, LDPE 42.7 [47,48], PEEK 4.07 nm, PA6-E 13.9 nm, POM-C 31.1 nm, PP 46.6 nm and PTFE 53.2 nm [49]. These parameters are used for different applications, and some of the 3D parameters are developed for 3D surface studies [50]. A summary of those parameters is reported in the literature [51] ISO25178.

Moreover, in materials science, optical microscopy is of limited use for imaging nanostructures. Thus, electron microscopy, EM, has been adopted to improve the resolution by taking advantage of the

sub-nanometer wavelength of electrons. However, EM is typically expensive and requires special sample preparation in a vacuum environment, which can irreversibly damage the sample. Photo-acoustic microscopy [55-61] has been developed as an imaging tool to capture strong optical absorption contrasts via the photoacoustic, PA, effect. PA transduction from optical excitation to acoustic emission is based on optical absorption and the consequent thermoelastic expansion of the sample. Recently, PA subdiffraction imaging has been introduced, based on either optical saturation or photo-bleaching [62]. The lateral resolution is still limited to the subdiffraction scale, however, and the optical excitation energies are still too high to invoke non-linear optical effects.

Recently, AFM has been developed for nanoscale investigations of polymers, including life science applications [63]. The use of this technique for the study of polymers has been widely diffused since the cost and maintenance of the equipment is inferior to that of modern electron microscopes, and additional information on the surface of polymers, such as, morphology, and surface roughness, can be obtained.

Given these advantages, AFM became widely used for research in such diverse fields as physics, biology, chemistry, medicine and materials science [64]. AFM has been more actively employed in this field [47] because the measurement can be done at atmospheric pressure and it is not necessary to pre-treat the specimen compared with Scanning Electronic Microscopy, SEM, where the specimen has to be gold-coated. Figure 1 (a) illustrates the components of the atomic force microscope, while Figure 1 (b) shows te photograph of the Atomic Force Microscope Model XE-100 of the brand Park Systems used to analyze the topography of the samples.

The image obtained results from the convolution of the real topography of the sample with the shape of the peaks and valleys generated by the vertical displacement of the tip during the scanning [47,48]. Contaminant layers can influence on the cantilever during scan, and results in a non proper resolution [65]. During the scan, frequencies from 50.000 to 500.000 cycles per second can be applied, however, the reduction in oscillation amplitude owing to friction, can be used to identify and measure surface features [65].

In addition to providing real 2D/3D information on the surface topography, the atomic force microscope works in diverse environ-

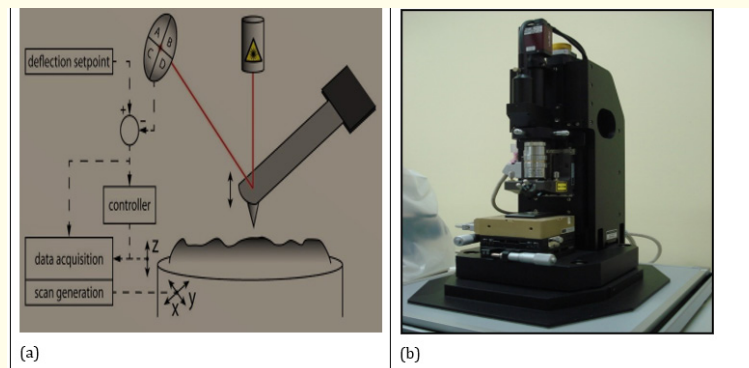


Figure 1: Schematic of: (a) mode of image acquisition using the atomic force microscope; (b) Photograph of the Atomic Force Microscope Model XE-100 of the brand Park Systems used to analyze the topography of the samples.

ments, such as in open air, under vacuum, at high pressure, under diverse atmospheres (e.g. inert gas surroundings) at different temperatures and humidities, and in liquids. AFM measures not only the surface topography but also a large number of surface properties, such as friction, electrical conductivity/resistance, thermal conductivity/resistance, glass transition temperature, melting temperature, stiffness, Young's modulus, adhesion, surface potential, capacitance, magnetism, electrochemistry parameters [66], or even coupled to the infrared spectroscopy (AFM-IR), to overcome size limitations [66]. This method combines simultaneous single particle measurements of physical properties such as hygroscopicity [67], surface tension [60,68], phase and morphology [70].

AFM has also been used to study R of polymeric membranes [71]. It is reported that the mean roughness of the membrane (measured by AFM) was directly proportional to the permeability of gases with the exception of Poly(*p*-phenylene oxide), PPO, $(C_8H_8O)_n$, membrane. The roughness parameter for PPO membrane was very low in comparison with other studied membranes. Gould., *et al.* [72] studied the surface of PET films and reported that the surface roughness can distinguish between the amorphous and crystalline regions. They also suggested that irregularities on the surface could affect the physico-chemical properties of the film. Diertz., *et al.* [73] reported the AFM images of polymeric membranes.

Fritzcheet., *et al.* presented AFM images of poly(vinylidene fluoride) membranes [74], poly(ether sulfone) membranes [75,76]

and poly(acrylonitrile) [77] membranes. In these studies, it was reported that the characteristics of membranes were reasonable regarding pore sizes between 0.0279 to 0.412 μm , and also, the pore size distributions of the membranes were acquired. The authors also suggested that AFM could provide information on the structure and shape of pore apertures. It was observed that the morphology of the surface on the membrane depends on the temperature used for the preparation of the membranes in PPO using 1,1,2-trichloroethylene, TCE as a solvent. The polarity of the solvent changed the permeability of the film. Thus, the morphology of the surface may have a role in material transport. Recently, a great deal of attention has been given to the morphology of the membrane surfaces and an attempt has been made to correlate the surface characteristics with the performance of the polymeric membranes [78]. In fact, AFM allowed the detection of characteristic differences in the surface morphology of different cellulose-based membranes in a state where preparation artifacts could be excluded [71].

In a morphological study of membranes using AFM, the phase shift can be measured, and it is derived from the difference in phase angle between the freely oscillating cantilever in air and the cantilever oscillation during scanning. The phase shift is zero when there is no interaction between the tip or the cantilever and the sample surface. However, in the case of a tip-sample interaction, a phase lag is induced if the interaction is attractive and a phase advance appears if the interaction is repulsive.

In polyethersulfone substrates, it was reported, a smaller interaction with the tip, resulting in a small phase shift. A larger phase shifts, exhibit high interaction between the tip and the membranes made of polyamide [65]. Experiments using hydrophilic Si tip, one can observe whether the interaction between the tip and the sample is hydrophilic or hydrophobic. Then, hydrophilic surfaces usually, interacts strongly with a hydrophilic tip, resulting in a large phase shift, or vice-versa [65].

Moreover, changes of relative homopolymer proportion in polymeric blends may vary the domain structure, being useful or necessary, a morphology study by AFM. In practice, the use of phase separation can be prone to make coatings, whose surface properties are different from the bulk [79].

AFM examination permit measuring different geometries on the sample surfaces, and a considerable number of related parameters. R size and shape definition are essential for quality control of final products, in addition many physical properties are affected; therefore, a precise description of R is needed [79].

Experimental

Plasma treatment system

The experimental setup used consists of a stainless-steel vacuum chamber (measuring 15 cm of diameter and 30 cm in height) with two horizontal parallel-plate circular internal electrodes of equal dimensions (11 cm in diameter), separated by 11 cm. The polymeric samples were set on the lower electrode and the system was evacuated by a rotary pump, model EM-18 from Edwards (18 m³/h), down to a pressure of ~ 2,66 Pa. Needle valves of nylon were employed to control the gas feeds (both of high purity: ~ 99.995%), and a capacitive pressure sensor, model Pirani, to monitor and to control the pressure inside the chamber. Samples of PVC, PET from a 2 L Coke bottle and LDPE from Dow Company, all measuring (2.5 cm × 1.5 cm) were exposed directly to the plasma atmosphere established by the application of radiofrequency power (13.56 MHz) coupled via a matching box circuit from Tokyo Hi Power [81,82].

A high voltage source GBS-Elektronik GmbH, RUP 6-20 with adjustable pulse magnitude from 0 to 20 kV was used for PIII technique. In some series of treatments on polymers negative pulses of -2400 V were also applied to the sample-holder electrode, while

the radiofrequency was applied to the upper electrode. Negative voltage pulses and pulse widths (or duration) were monitored at a frequency of 300 Hz using a Tektronix TDS 2014 digital oscilloscope [47,48]. In this section are reported AFM images obtained using a Park Instruments 100-00 microscope of commercial polymers PVC, PET and LDPE, and R_{rms} were calculated.

Examination using AFM

The examination was made using a 100-00 atomic force microscope from Parker system, (Suwon, South Korea) consisted of a flexible rod in the lower part of which there is a tip with a dimension of a few micrometers of height. Under this tip, there is a Silicon Nitride, SiN, responsible for the interaction with the atoms or molecules of the polymeric samples (PVC, PET and PE). To traverse the sample to obtain an image, a positioning system based on piezoelectric ceramics, capable of performing movements in three dimensions (xyz), with angstroms (Å) precision is used. During scanning, a laser beam alignment system was also used, which focuses on the lever and reflects on a four-quadrant sensor. The sensor provides deflection information to the feedback and control system, which corrects the position of the lever to maintain an interaction with the sample during the scan, and to obtain the image (5 μm × 5 μm) or (10 μm × 10 μm of area, in non-contact mode for 27 polymeric samples of PVC, PET, PE and Polyamide. In this mode the tip moves about 50–150 Å above the sample surface. The attractive forces from the sample are substantially weaker, near to (10⁻¹³ N) in non contact mode. The cantilever is driven to vibrate near its resonant frequency of 256 Hz by a piezoelectric element.

Characterization of surface roughness involved two steps: instrumental measurement and quantification of the heights and lateral dimensions. Surface roughness characterization can be based on the correlation analysis for both, roughness heights and lateral dimensions [79]. Applications could also have included the identifying in transitions between different components on polymeric samples [80].

Results and Discussions

Figure 2 shows AFM images of PET, and of ZnO films deposited by radiofrequency magnetron sputtering under different conditions. A Park Instruments 100-00 was used to obtain the images. These films find opto-electronic applications.

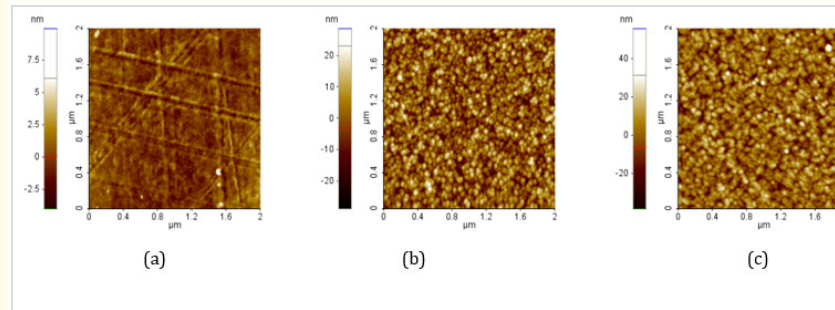


Figure 2: In (a) pristine PET, a courtesy of NetPrint company - $R_{\text{RMS}} = 1.04 \text{ nm}$; (b) ZnO deposited by 60 min. - $R_{\text{RMS}} = 7.34 \text{ nm}$; (c) ZnO deposited by 120 min. - RRMS = 9.37 nm. The other parameters were 100 to 110 °C, rf power 70 W, 10 mTorr of Ar + O₂ in equal proportion using rf magnetron sputtering.

Courtesy of Dr. José Roberto Ribeiro Bortoleto, Technological Plasmas Laboratory, UNESP, Sorocaba-SP, Brazil

Note that the surface of the film is formed by a continuous and homogeneous distribution of grain-like structures. In addition, as deposition time and thickness increase, these structures continually grow in size and height. The aspect of AFM images containing film is totally different from pristine PET, or PET treated with reactive gases, i.e. sulfur hexafluoride or nitrogen. We suggest the use of sample holder cooler system during oxide thin films deposition on transparent polymer substrates, because it does not

resist temperatures above 100°C, or even for deposition times > 120 min. We also suggest that some heating occurs owing to ion bombardment, and collisions with electrons and neutral species.

Moreover, we introduce AFM images taking 5 μm × 5 μm of area of commercial Poliamide. In a, the pristine polymer, and in b, with zinc oxide thin film deposited by rf sputtering, at 2 mTorr O₂, 1 mTorr Ar, at 409 V, 1.1 mA for 20 min.

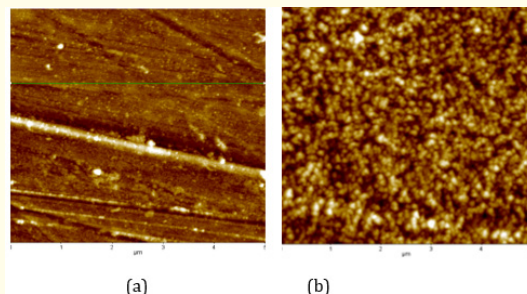


Figure 3: In (a) pristine polyamide, - $R_{\text{RMS}} = 7.02 \text{ nm}$; (b) ZnO RRMS = 93.09 nm.

Courtesy of Dr. José Roberto Ribeiro Bortoleto, Technological Plasmas Laboratory, UNESP, Sorocaba-SP, Brazil.

Note that the surface of polyamide possess smooth surface containing aligned polymeric chains few intense peaks, although the presence of risks in some directions well defined, owing to the process fabrication and cleaning. On the other hand, ZnO film is formed by a continuous and homogeneous distribution of grain-like struc-

tures. The aspect of AFM images containing film is totally different from pristine polyamide. We suggest the short deposition times (~20 to 30 min.) aiming the polyamides can resist temperatures above 100°C. We also suggest, again, that some heating occurs owing to ion bombardment, and collisions with electrons and neutral species.

Figure 4 shows the AFM images of the pristine substrates of white PVC, 2L CokeTM bottle PET and LDPE from DOW Company. The images were obtained using a XE-100-00 Atomic Force Microscope from Park Instruments. The area scanned was $10 \mu\text{m} \times 10 \mu\text{m}$ in the non-contact mode.

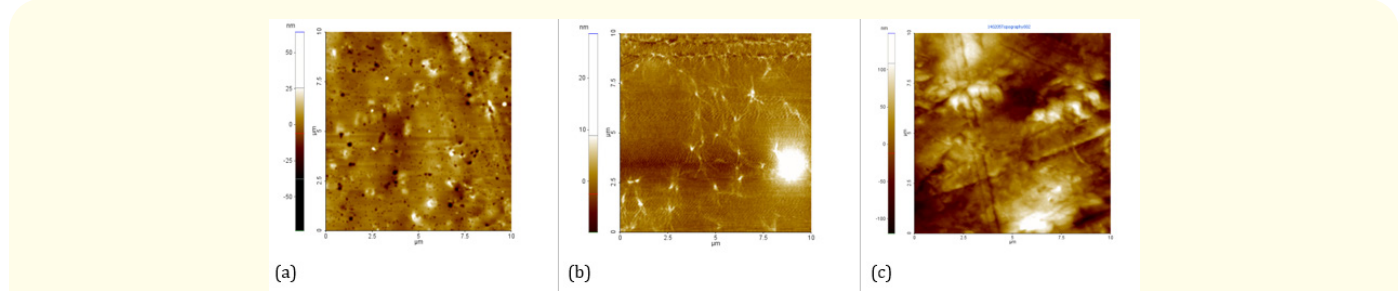


Figure 4: AFM images ($10 \mu\text{m} \times 10 \mu\text{m}$) of PVC, PET and PE. In (a) the R_{rms} roughness of the PVC was 4.38 nm ; (b) the R_{rms} roughness of PET was 1.79 nm ; (c) the roughness R_{rms} of the LDPE was 42.7 nm . Reproduced with permission [47,48]. Copyright [2018] Scholar's press.

depths up to tens of nanometers, representing at least an order of magnitude higher than the average roughness of the PVC. The R_{rms} roughness was 4.39 nm . Contact angle of this sample was $70 \pm 4^\circ$. In Figure 4 (b) the AFM image of the virgin PET is observed, which in turn is characterized by the alignment of the fibers and the absence of pinholes. The rms roughness of PET was 1.79 nm . Contact angle of this sample was $66 \pm 5^\circ$. Figure 4 (c) shows the AFM image of the virgin PE, whose irregular topography reveals risks in different directions and depths that may have been produced due to the cleaning process. The R_{rms} roughness of the PET was 42.7 nm . Contact angle of this sample was $74 \pm 1^\circ$. White shadows in images represent peaks or higher regions of polymeric chains, while darker regions represent the valleys.

According to Figure 4, white shadows in images represents peaks or higher regions of polymeric chains, while darker region represents the valleys, and also, a high density of pinholes is observed for virgin PVC due to the absence of polymer chains in these regions. It is observed from the scale that these holes have

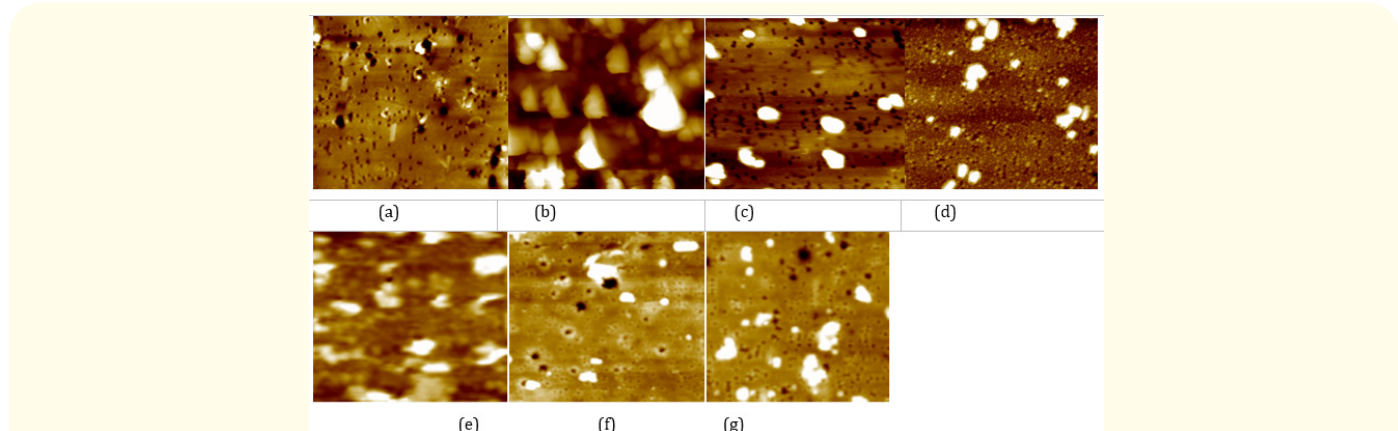


Figure 5: Pictures of PVC treated by SF6 Plasma (a) untreated, $R = 7.8 \text{ nm}$ (b) 25 W , PI cathode, $R = 4.7 \text{ nm}$ (c) 25 W , PI anode, $R = 2.6 \text{ nm}$ (d) 25 W , PIII, $R = 2.5 \text{ nm}$ (e) 100 W PI cathode, 49.5 nm (f) 50 W , PIII, 6.1 nm (g) 100 W , PIII, $R = 12.6 \text{ nm}$. PIII parameters were: -2400V , $30 \mu\text{s}$, 300 Hz .

surface is small and not aggressive enough to rough the surface. R in this case is 4.7 in PI cathode, 2.6 nm in PI anode and 2.5 nm in PIII. Increasing rf power, at 50 W, samples presented higher roughness: 6.1 nm. Increasing even more rf power, at 100 W, roughness increased considerably, reaching 12.6 nm in PIII and 49.5 nm in PI cathode. Hence, the PVC surface is very sensitive to rf power and electrical configuration of the reactor. Bombardment using SF₆ gas promotes distinctive degrees of shocks and physical collision between S and F ions on polymeric chains of PVC. In PIII, ions tend to

reach some tens of nanometers under the top layers of C-H \circ C-Cl covalent bonds (forming considerably rigid chains, but sensitive to high acceleration of ions towards itself).

Figure 6 introduces AFM images of PVC treated with 6.56 Pa of nitrogen plasmas at 25 to 100 W for 300 s for different plasma immersion techniques. Parameters of PIII were: - 2400V, 30 μ s, 300 Hz.

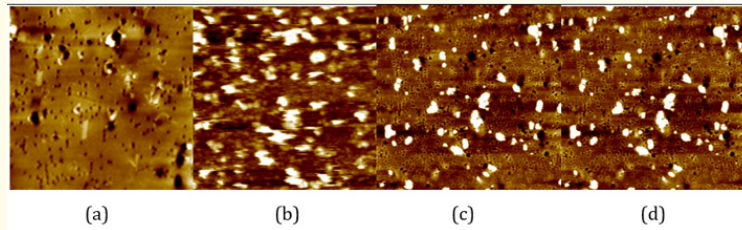


Figure 6: Pictures of PVC treated by N₂ Plasma (a) untreated PVC, R = 7.8 nm (b) 100 W, PI cathode, R = 4.4 nm (c) 75 W, PIII, R = 1.4 nm (d) 75 W, PIII, R = 1.7 nm. PIII parameters were: -2400V, 30 μ s, 300 Hz.

In relation to PVC treated by plasma immersion techniques in figure 6, using N₂ plasmas; note there was a slight decrease of roughness. Nitrogen ion bombardment of the surface is moderate and does not cause deformations of the surface, even in PI cathode, in which ions shock the surface constantly. The cross-links between the neighboring polymer chains reduced the presence of pinholes. Owing to ion bombardment, peaks on surface are easily broken, and the surface of PVC becomes smoother.

The AFM images of PET samples before and after the plasma treatment with SF₆ is shown in figure 7 and using nitrogen is shown in figure 8. In both cases, 6.56 Pa of Nitrogen for 300 s at 25 to 150 W was used with different Plasma Immersion techniques [85,86].

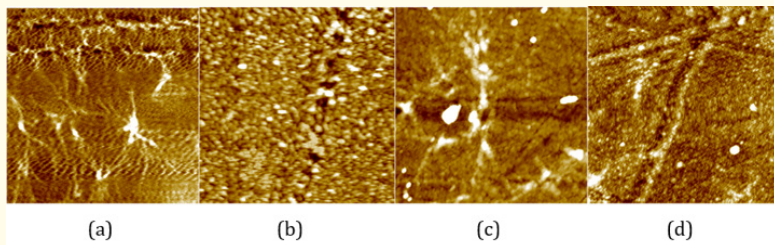


Figure 7: Pictures of PET treated by SF₆ Plasma (a) untreated, R = 1.8 nm (b) 100 W, PI cathode, R = 4.7 nm (c) treated with 6.56 Pa, 25 W, PIII, R = 2.6 nm (d) 150 W, PIII, R = 2.5 nm. Parameters of High Voltage: - 2400V, 30 μ s, 300 Hz. Reproduced with permission.85

Copyright [2018] Medwin publisher.

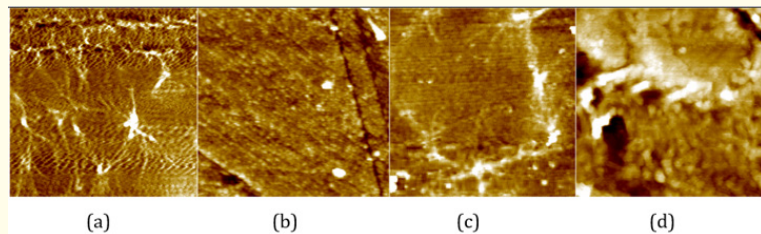


Figure 8: Pictures of PET treated by N2 Plasma (a) untreated, $R = 1.8$ nm (b) 100 W, PI, $R = 4.4$ nm (c) 75 W, PIII, $R = 1.4$ nm (d) 75 W, PIII, $R = 1.7$ nm. Parameters of High Voltage: - 2400V, 30 μ s, 300 Hz. Reproduced with permission.85 Copyright [2018] Medwin publisher.

The AFM images reveal that the surface of the PET substrates is relatively smooth, that is, it presents a more regular morphology than the morphology of the PVC samples. In fact, the R_{rms} of the PET was 1.8 nm for these AFM images. In addition, the PET surface is free of pinholes. In addition, the PET substrates, contain aromatic rings and double bonds, and they are therefore, more rigid, in which, presents greater resistance to the ionic bombardment during the plasma treatment, and the morphological changes induced by the plasma kinetics are more subtle, consequently, the R_{rms} roughness values were in fact smaller than the PVC roughness values. Again, in PIII ions tend to lodge some tens of nanometers under the top layers of the polymeric chains, being an effective mechanism to control R . During the plasma phase, the ions accelerated towards the surface usually to break the peaks, thus reducing R_{rms} . There are scratches inherent in the process of cleaning of PET samples [86].

In addition, there is strong relationship between wettability and surface roughness. The degree of wettability of the samples after treatment has its effect amplified when R is higher, because a larger area available can support more chemical bonds on the surface. Moreover, in ion implantation, the degree of bombardment and the resulting temperature increase become significant in increasing the distance of atoms, weakening the strength of connections and thus promoting greater tendency to break chemical bonds on peaks of the surface. As long as the surface energy increases, free radicals tend to link to the atmospheric oxygen, especially after breaking the vacuum, in which oxygen-containing groups and other polar radicals can recombine on the surface by hydrogen bonds [82].

For the nitrogen treatment, polar functional oxygen groups on the surface usually reduces θ . Since the potential energy of oxygen groups is the highest among the particles available in the plasma, the functionalization is often attributed to radicals containing oxygen when they recombine on the surface of a given polymer, being possible to induce the etching of polymeric materials, mainly on the amorphous region [82], or even into the less resistive component of the polymeric substrates [87].

In PIII, ions are implanted into the polymeric matrix, occupying in their vacancies. If we consider that the concentration of ions in plasma is 5 orders of magnitude lower than the neutral particles, plasma is rarefied. Considering also that the PIII under this condition does not change its shape and roughness values significantly, it seems that the pulse applied has less or no effect compared to the power [82].

It is not obvious that the new surface morphology induced by plasma treatment is not sufficient to contribute to the improvement of the hydrophobicity by the known "Lotus effect". Essentially, droplets can achieve a smaller contact area being supported at the top of the sharp features of the surface, minimizing the interaction energy. It is known that the structured surface of many water-repellent leaves consist of elevations in until near to 100 μ m and the distance between the elevations can reach about 200 μ m. Owing to the different order in the height and the distance compared with the size of water drops, it is clearly seen that the Lotus effect is not the main reason for the improved hydrophobicity for PVC and PET treated with SF_6 plasmas, on the improvement of hydrophilicity for PVC and PET samples treated with nitrogen plasmas [88].

The necessary conditions for hydrophilic PET do not allow a detailed hypothesis on the interaction between reactive particles of low energy, since the potential energy of oxygen groups and the functionalization of a polymer surface may be associated with those radicals, which changes the evolution of the morphology on the polymer surfaces [82].

These results indicated that the generation of new functional polar groups may affects the surface sorption. For further studies, correlations of the gas penetration with new polymer elements should be investigated [89], when the changes in R are near to the pristine PET.

It was observed also that fluorine plasma treatments even in low energy, usually produce etching of species [90]. According to the literature, plasma treatment leads to alterations of the polymer surface properties, the significance of the changes being dependent on the polymer species. Thanks to high ablation rate, very significant changes are observed on PTFE. It can be supposed that PTFE amorphous phase is ablated faster than crystalline one [91]. Faster ablation of amorphous phase was reported also for high density PE. Preferential ablation of PE results in creation of lamellar structures reflecting arrangement of molecular chains on the PE surface [92]. In other polymers with lower crystalline fraction (PP, PET, PS) the tiny, sharp formations appearing after the plasma treatment may represent low molecular, oxidized structures [93]. Plasma treatment does not change the surface morphology of PET and PS dramatically with only exception of formation of minor surface folding (rippling, wrinkling). Similar result was reported, in [94,95].

Other common process is the degradation of the polymer surface, which causes a change in the surface topography that can be evaluated by AFM analysis. This reveals a slight increase in surface roughness, as occurred with LDPE treated by oxygen plasmas, and may be attributed to surface degradation/etching a due to ion bombardment, and it can be able to change the crystallinity of the treated polymer [96], and then, carbonyl, carboxyl or hydroxyl groups may be produced [96]. In that case, R_{rms} of pristine LDPE was 21.05 nm, while treated LDPE presented an R_{rms} of 21.85 nm for 600 s of exposure time, $R = 24.58$ nm for 1200 s and $R_{rms} = 29.89$ nm for 1800 s.

Another polyolefin, polypropylene, PP, is relatively smooth, $R_{rms} = 36.0$ nm, showing an annular and granular structure of the natural shape when it is bi-oriented. These structures were totally dispersed on the surface. The difference between the highest and the lowest peak on the line is around 50 nm. This topography is dominated by annular protrusions with boundaries between them clearly visible. O_2 plasma treatment etches the surface of PP, forming aggregates on the surface. In exposure time of only 30 s, $R = 44.06$ nm. With further increase of the exposure time (180 s) and more plasma power, the surface becomes rougher, $R = 69.1$ nm, where the annular features previously found on the untreated sample surface, care changes to a randomly-shaped. This illustrates large number of nano-scale depressions formed on the sample surface following plasma treatment. This modification in the surface morphology is thought to result mainly from the bombardment of the surface by the energetic particles present in the plasma [97]. While using Argon plasma treatment, the etching effect makes the surface of the PP even rougher, reaching $R = 49.5$ nm for 30 s and $R = 60.8$ nm for 180 s. Argon plasma treatment is reported in the literature [97].

With increasing time of the plasma treatment the total oxygen content in the polymer surface layer increases [98]. Creation of the oxidized structures has been proven before on the plasma treated polyolefins [99,100]. Owing to the plasma treatment, unpaired spins (i.e. free radicals) are generated on the polymer molecular chain. Not only C-H but also C-C, C-F and "new" C-O bonds are likely to break. The bond breaking leads to fragmentation of the polymer chain and to ablation of polymer surface [101].

Finally, the literature reports several advanced research results using AFM and new perspectives for the micro-nano science community to operate in different areas of materials such as polymers and summarizes their methods and related technologies [102]. In other studies, PTFEMA and PMAA films have been treated to test their water spill and aging. The morphology study of these treated polymer films were examined using AFM [103].

Moreover, nanoparticles were synthesized in a variety of sizes from 10-1000 nm, requiring nanoscale methods such as scanning probe microscopy for sizing and morphology mea-

surements. Using an AFM operating in vibrating mode under ambient conditions, the authors successfully characterized both the shape and size of their polymer nanoparticles synthesized from polymers of different molecular weight [104].

In a study of Epoxy resin, which was modified by the incorporation of PCL–PDMS–PCL triblock copolymer (TBCP) in the presence of DDM. The morphology of the Epoxi resin was evaluated by AFM and, after processing, nanoscale inhomogeneities produced an average roughness of 20 nm [105].

In another study, multifunctional monomers including hexane-diol diacrylate (HDDA) and a hybrid acrylate-oxtane monomer (OXMA) were incorporated to modify the domain size scale and phase-separated morphology of a butyl acrylate (BA) and difunctional oxtane (DOX) system. Photopolymerization of the DOX/BA system results examined by AFM reveal the distinct and co-continuous soft acrylate and hard oxtane domains. Incorporating different amounts of HDDA or OXMA generates polymer morphologies with smaller, continuous, hard domains because of the reduction in time difference between the onset of phase separation [106]. These results demonstrate that phase separation and polymer morphology in radical/cationic systems can be directed using multi-functional monomers enabling enhancements in mechanical properties including tensile toughness and impact strength. The addition of a crosslinker significantly increases the T_g of acrylate-rich domain as much as 45 °C, forming less distinct and broad peaks on its surface [106].

AFM has also been used to evaluate the surface properties of chitosan hydrogels, which depend on parameters such their concentration (1.5%, 2.5% and 3.5%), their degree of acetylation (4% and 38.5%), and the conditions of the gelation process. Chitosan hydrogels represent a family of natural polymers exhibiting several exceptional properties [107]. Chitosan-hybrid nanocomposites were applied to bone regeneration, and the effect of POSS (smallest silica particle) nanocages on surface, morphology, structure and *in vitro* bioactivity assessed. POSS incorporation altered R [108].

In all cases, AFM is an indispensable technique for characterization of polyolefins and other polymers, such as shape memory polymers (SMPs) and polymer blends.¹⁰⁹ More specifically, PLA/PBS/PBAT blends were also evaluated by AFM [110]. The studies

show that the morphology changes different components making the contributions to the improvement of mechanical and other properties [110]. Given every example in this chapter, we emphasize the use AFM as necessary and useful for morphology or roughness studies of polyolefins or degradable polymers [110]. In general, variations in the morphology of polymer resulted from different growth mechanisms, which depend on the properties of the coated compound, and the treatment conditions. Given every example in this chapter, we emphasize the use AFM as necessary and useful for morphology or roughness study for polyolefin's in or degradable polymers [111].

Moreover, the coupling of AFM-IR provides another advantage and thus, helps to the study of polymeric samples. One example is the recent progress in the application of AFM and AFM-IR to enhance its resolution. It was also discussed the latest progress in the use of AFM-IR for the chemical analysis of polymer materials dealing with polymer composites, blends, multilayers, or biopolymers [112]. Finally, it was demonstrated how AFM-IR could be used to determine phase separation and crystallization at nanoscales [112].

Further, the surface of the polypropylene film was functionalized via UV grafting (365 nm) of GMA in the presence of benzophenone into the methanol or mixed solvents (methanol and water). The addition of 40 v/v% of water into the coating solution led to an increase in grafting density, a reduction in UV-irradiation time, and changes in the grafting morphology. AFM was also used in the identification of the array structure configuration on the surface of the polymeric films [113].

A restriction is concerned to the type of organic solvents used in interfacial polymerization affects the surface property, free volume, and separation performance of the thin-film composite (TFC), i.e., in polyamide membrane. Hence, AFM can be essential for surface morphology of this type of material, as suggested for further studies [114].

In general, variations in the morphology of polymers films and polyolefin's on different surfaces were explained by diverse growth mechanisms and conditions, and a lot of new experiments are still in progress, as recommended for future studies.

Conclusions

Polymers have been used successfully in fields. In general, special surface properties with regard in various fields. They have excellent bulk physical and chemical properties, and are inexpensive and easy to process. For these reasons, surface modification techniques which can transform these advantageous materials into highly valuable finished products have become an important part of the plastics industry [115-119].

AFM is one of the foremost tools for imaging, measuring, and manipulating the surface of materials at the nanoscale, and has a resolution on the order of nanometers, much better than the optical diffraction limit. Recently, the use of this technique for the study of polymers has been widely diffused as the cost and maintenance of the equipment is inferior to that of modern electron microscopes. Additional information on the surface of polymers, such as morphology and surface roughness, can be obtained, as well as magnetic, mechanical, thermal and optical data. In general polymers are smooth presenting roughness lower than 30 nm.

Acknowledgments

The authors are grateful to Brazilian agencies, CAPES, CNPq and FAPESP for all support.

Bibliography

1. Schlüter S., et al. "Pore-scale displacement mechanisms as a source of hysteresis for two-phase flow in porous media". *Water Resources Research* 52.3 (2016): 2194.
2. Geistlinger H., et al. "Impact of surface roughness on capillary trapping using 2D-micromodel visualization experiments". *Transport in Porous Media* 112.1 (2016): 207.
3. Moreno L and Babadagli T. "Multilayer organic deposition on the rock surface with different wettabilities during solvent injection for heavy-oil recovery". *The Canadian Journal of Chemical Engineering* 93.4 (2015): 664.
4. Svorcík V., et al. "From gold nano-particles through gold nano-wire to gold nano-layers on substrate". In: Chow PE, editor. *Gold nanoparticles: properties, characterization and fabrication*. Nova Sci. Publ: New York. 1 (2010).
5. Acáková L and Svorcík V. "Cell colonization control by physical and chemical modification of materials". In: Kimura D, editor. *Cell growth processes: new research*. Nova Sci. Publ. New York, 5 (2008).
6. Inagaki N. "Plasma-Surface Modification and Plasma Polymerisation, Technomic, Lancaster". CRC Press, Boca Raton, PA, 1 (1995).
7. Lai J., et al. "Study on hydrophilicity of polymer surfaces improved by plasma treatment". *Applied Surface Science*, Amsterdam. 252.10 (2006): 3375.
8. Choi Y., et al. "Characteristics of atmospheric pressure N₂ cold plasma torch using 60-Hz AC power and its application to polymer surface modification". *Surface and Coatings Technology* 193.1-3 (2005): 19.
9. Kotál V., et al. "Gold Coating of Poly (ethylene terephthalate) Modified by Argon Plasma". *Plasma Processes and Polymers* 4:69 (2007).
10. Boyd RD., et al. "Atmospheric Nonequilibrium Plasma Treatment of Biaxially Oriented Polypropylene". *Macromolecules* 30 (1997): 5429.
11. Rockova K., et al. "Bio-compatibility of ion beam-modified and RGD-grafted polyethylene". *Nuclear Instruments and Methods in Physics Research Section B* 225.3 (2004): 225.
12. Švorcík V., et al. "Adhesion and proliferation of keratinocytes on ion beam modified polyethylene". *Journal of Materials Science: Materials in Medicine* 11 (2000): 655.
13. Svorcík V., et al. "Modification of surface properties of high and low density polyethylene by Ar plasma discharge". *Polymer Degradation and Stability* 91.6 (2006): 1219.
14. Tahara M., et al. "Improvement in adhesion of polyethylene by glow-disc harge plasma". *Surface and Coatings Technology* 174-175 (2003): 826.
15. Gerenser L J. "XPS studies of in situ plasma-modified polymer surfaces". *Journal of Adhesion Science and Technology* 7 (1993): 1019.

16. Selli E., et al. "Synthesis and characterisation of end-functionalised poly (N-vinylpyrrolidone) additives by reversible addition-fragmentation transfer polymerization". *Journal of Materials Chemistry* 11 (2001): 1985.
17. Hegemann D., et al. "Plasma treatment of polymers for surface and adhesion improvement". *Nuclear Instruments Methods B*. 208 (2003): 281.
18. Maddison DS and Unsworth J. "Optimization of synthesis conditions of polypyrrole from aqueous solutions". *Synthetic Metals* 30.1 (1989): 47.
19. Balu B., et al. "Fabrication of "Roll-off" and "Sticky" Superhydrophobic Cellulose Surfaces via Plasma Processing". *Langmuir* 24.9 (2008): 4785.
20. Beake BD., et al. "Scanning force microscopy investigation of poly (ethylene terephthalate) modified by argon plasma treatment". *Materials Chemistry* 8 (1998): 1735.
21. N Vandencasteele., et al. "Selected Effect of the Ions and the Neutrals in the Plasma Treatment of PTFE Surfaces: An OES-AFM-Contact Angle and XPS Study". *Plasma Processes and Polymers* 2.6 (2005): 493-500.
22. Teshima, K., et al. "Ultra-Water-Repellent Poly (ethylene terephthalate) Substrates". *Langmuir* 19.25 (2003): 10624.
23. Powell H M and Lannutti JJ. "Nanofibrillar Surfaces via Reactive Ion Etching". *Langmuir* 19.21 (2003): 9071.
24. Di Mundo R., et al. "Influence of Chemistry on Wetting Dynamics of Nanotextured Hydrophobic Surfaces". *Langmuir* 26.7 (2010): 5196.
25. Leitel R., et al. "Broadband Antireflective Structures on PMMA by Plasma Treatment". *Plasma Processes and Polymer* 4 (2007): 878.
26. Youngblood J P and McCarthy T. "Ultrahydrophobic Polymer Surfaces Prepared by Simultaneous Ablation of Polypropylene and Sputtering of Poly (tetrafluoroethylene) Using Radio Frequency Plasma". *Journal of Macromolecules* 32.20 (1999): 6800.
27. Manca M., et al. "Influence of Chemistry and Topology Effects on Superhydrophobic CF₃-Plasma-Treated Poly (dimethylsiloxane) (PDMS)". *Langmuir* 24.5 (2008): 1833.
28. Tsougeni K., et al. "Control of Nanotexture and Wetting Properties of Polydimethylsiloxane from Very Hydrophobic to Super-Hydrophobic by Plasma Processing". *Plasma Processes and Polymers* 4 (2007): 398.
29. Tserepi A., et al. "Nanotexturing of poly (dimethylsiloxane) in plasmas for creating robust super-hydrophobic surfaces". *Nanotechnology* 17 (2006): 3977.
30. Morber JR., et al. "Wafer-Level Patterned and Aligned Polymer Nanowire/Micro- and Nanotube Arrays on any Substrate". *Advances in Material* 21 (2009): 2072.
31. Powell HM., et al. "Nanotopographic Control of Cytoskeletal Organization". *Langmuir* 22.11 (2006): 5087.
32. Northen M T and Turner K L. "A batch fabricated biomimetic dry adhesive". *Nanotechnology* 16 (2005): 1159.
33. Koch K and Barthlott W. "Droplets on Superhydrophobic Surfaces: Visualization of the Contact Area by Cryo-Scanning Electron Microscopy". *Philosophical Transactions of the Royal Society A* 367 (2009): 1487.
34. Guo Z and Liu W. "Biomimic from the superhydrophobic plant leaves in nature: Binary structure and unitary structure". *Plant Science* 172.6 (2007): 1103.
35. Barthlott W and Neinhuis C. "Purity of the sacred lotus, or escape from contamination in biological surfaces". *Plant Science* 202.1-8 (1997): 1.
36. Li Y and Liu F. "A facile layer-by-layer deposition process for the fabrication of highly transparent superhydrophobic coatings". 19 (2009): 2730.
37. Yang C., et al. "Effect of upper contact line on sliding behavior of water droplet on superhydrophobic surface". *Chinese Science Bulletin* 54 (2009): 727.
38. d'Agostino R., et al. "Plasma Processes and Polymers". 3. Wiley VCH: New York, (2005).

39. Järnström J., et al. "Roughness of pigment coatings and its influence on gloss". *Applied Surface Science* 254.18 (2008): 5741.
40. Li J., et al. "In situ AFM study of the surface morphology of polypyrrole film". *Synthetic Metals* 74.2 (1995): 127.
41. Lee EH., et al. "Effects of electronic and recoil processes in polymers during ion implantation". *Journal of Materials Research* 9.4 (1994): 1043-1050.
42. Sant'Ana PL. "Polímeros tratados a plasma para dispositivos e embalagens". Novas edições acadêmicas, 1 (2019).
43. Sant'Ana PL. "Polymers Treated By Plasma For Optical Devices And Food Packaging". Scholar's Press, 1 (2018).
44. Hayder Lateef Radhi Al-Maliki. "Adhesive and tribological behaviour of cold atmospheric plasma-treated polymer surfaces". Szent Istvan University, *Gödöllő*, 1 (2018).
45. Stout K J., et al. "The development of methods for the characterization of roughness in three dimensions". *Commission of the European Communities* 1 (1993).
46. Blunt L and Jiang X. "Advanced techniques for the assessment of surface topography, Development of a basis for 3D surface texture standards "SURFSTAND". Chapter 2.1 (2003): 355.
47. Miyoshi K. "Surface Characterization Techniques: An Overview". NASA Technical Report NASA/TM-2002-211497 (2013).
48. Raghavendra N V and Krishnamurthy L. "Metrology of surface finish, in Engineering Metrology and Measurements (Oxford University Press)" Ch. 9. (2013).
49. Petropoulos GP., et al. "Surface Texture Characterization and Evaluation Related to Machining, in Surface Integrity in Machining". ed. J.P. Davim, Springer, Ch. 2 (2010).
50. Galanžha EI., et al. "In vivo magnetic enrichment and multiplex photoacoustic detection of circulating tumour cells". *Nature Nanotechnology* 4 (2009): 855.
51. Jathoul AP., et al. "Deep in vivo photoacoustic imaging of mammalian tissues using a tyrosinase-based genetic reporter". *Nature Photonics* 9 (2015): 239.
52. Pu K Y., et al. "Semiconducting polymer nanoparticles as photoacoustic molecular imaging probes in living mice". *Nature Nanotechnology* 9 (2014): 233.
53. Razansky D., et al. "Multispectral opto-acoustic tomography of deep-seated fluorescent proteins *in vivo*". *Nature Photonics* 3 (2009): 412.
54. Shelton R L., et al. "Volumetric imaging of erythrocytes using label-free multiphoton photoacoustic microscopy". *Journal of Biophotonics* 7 (2014): 834.
55. Wang L V and Hu S. "Photoacoustic tomography: *in vivo* imaging from organelles to organs". *Science* 335.6075 (2012): 1458.
56. Yao J J., et al. "High-speed label-free functional photoacoustic microscopy of mouse brain in action". *Nature Methods* 12 (2015): 407.
57. Yao J J., et al. "Photoimprint photoacoustic microscopy for three-dimensional label-free subdiffraction imaging". *Physical Review Letters* 112 (2014): 014302.
58. Ruggeri FS., et al. "Infrared nanospectroscopy characterization of oligomeric and fibrillar aggregates during amyloid formation". *Nature Communication* 6.7831 (2015): 1.
59. Khulbe KC., et al. "Surface morphology of homogeneous and asymmetric membranes made from poly (phenylene oxide) by tapping mode atomic force microscope". *Journal of Applied Polymer Science* 59 (1996): 151.
60. Boussu K., et al. "Roughness and hydrophobicity studies of nanofiltration membranes using different modes of AFM". *Journal of Colloid and Interface Science* 286 (2005): 632.
61. Dazzi A., et al. "AFM-IR: Combining Atomic Force Microscopy and Infrared Spectroscopy for Nanoscale Chemical Characterization". *Applied Spectroscopy* 66.12 (2012): 1365.
62. Morris HS., et al. "Quantifying the Hygroscopic Growth of Individual Submicrometer Particles with Atomic Force Microscopy". *Analytical Chemistry* 88.7 (2016): 3647.
63. Morris HS., et al. "Humidity-dependent surface tension measurements of individual inorganic and organic submicrometre liquid particles". *Chemical Science* 6.5 (2015): 3242.

64. Hritz A D., et al. "A method for the direct measurement of surface tension of collected atmospherically relevant aerosol particles using atomic force microscopy". *Atmospheric Chemistry and Physics* 16.15 (2016): 9761.
65. Krueger BJ., et al. "Formation of Microcrystals, Micropuddles, and Other Spatial Inhomogeneities in Surface Reactions under Ambient Conditions: An Atomic Force Microscopy Study of Water and Nitric Acid Adsorption on MgO (100) and CaCO₃ (1014)". *Langmuir* 21.19 (2005): 8793.
66. Khulbe KC and Matsuura T. "Characterization of synthetic membranes by Raman spectroscopy, electron spin resonance, and atomic force microscopy; a review". *Polymer* 41.5 (2000): 1917.
67. Gould SAC., et al. "Influence of substrate morphology on the cohesion and adhesion of thin PECVD oxide films on semi-crystalline polymers". *Journal of Applied Polymer Science* 65 (1997): 1237.
68. W R Nidal., et al. "Visualisation of an ultrafiltration membrane by non-contact atomic force microscopy at single pore resolution". *Journal of Membrane Science* 110.2 (1992): 229.
69. Fritzsche AK., et al. "The surface structure and morphology of polyvinylidene fluoride microfiltration membranes by atomic force microscopy". *Journal of Membrane Science* 68.1-2 (1992): 65.
70. Fritzsche AK., et al. "The structure and morphology of the skin of polyethersulfone ultrafiltration membranes: A comparative atomic force microscope and scanning electron microscope study". *Journal of Applied Polymer Science* 45 (1992): 1945.
71. Fritzsche AK., et al. "The surface structure and morphology of polyacrylonitrile membranes by atomic force microscopy". *Journal of Applied Polymer Science* 81.1-2 (1992): 109.
72. Fritzsche A K., et al. "Molecular dynamics simulations of the transport of water-ethanol mixtures through polydimethylsiloxane membranes". *Journal of Membrane Science* 38.5 (1997): 1031.
73. Khulbe K C., et al. "Characterization of Polyphenylene Oxide and Modified Polyphenylene Oxide Membranes". *Journal of Membrane Science* 135.2 (1997): 211.
74. Zukiene K., et al. "AFM lateral force imaging of modified polychloroprene: A study based on roughness analysis". *Applied Surface Science* 253 (2006): 966.
75. Dienwiebel M., et al. "Design and performance of a high-resolution frictional force microscope with quantitative three-dimensional force sensitivity". *Review of Scientific Instruments* 76 (2005): 043704.
76. Sant'Ana PL., et al. "Análise comparativa entre o grau de molhabilidade dos polímeros reciclados PVC e PET tratados por imersão ou deposição de filmes orgânicos em plasmas fluoreados". *Revista Brasileira de Aplicações de Vácuo* 37.3 (2019): 120.
77. Sant'Ana PL., et al. "Study of wettability and optical transparency of pet polymer modified by plasma immersion techniques". *Revista Brasileira de Aplicações de Vácuo* 16.2 (2017): 68.
78. He XM., et al. "Optical and tribological properties of diamond-like carbon films synthesized by plasma immersion ion processing". *Thin Solid Films* 355/356 (1999): 167.
79. Jinlong Z., et al. "Superhydrophobic of polymer films via fluorine atoms covalent attachment and surface nano-texturing". *Journal of Fluorine Chemistry* 200 (2017): 123.
80. Sant'Ana PL., et al. "Surface Properties and Morphology of PET Treated by Plasma Immersion Ion Implantation for Food Packaging". *Nanomedicine and Nanotechnology Open Access* 3 (2018): 1.
81. Sant'Ana P L., et al. "Surface Properties of PET Polymer Treated by Plasma Immersion Techniques for Food Packaging". *International Journal of Nano Research* 1 (2018): 33.
82. Jinlong Z., et al. "Superhydrophobic of polymer films via fluorine atoms covalent attachment and surface nano-texturing". *Journal of Fluorine Chemistry* 200 (2017): 123-132.
83. Chu PK., et al. "Third-generation plasma immersion ion implanter for biomedical materials and research". *Review of Scientific Instruments* 72.3 (2001): 1660-1665.
84. Guruvenket S., et al. "Plasma surface modification of polystyrene and polyethylene". *Applied Surface Science* 236.1-4 (2004): 278-284.

85. Triandafillu K., et al. "Adhesion of pseudomonas aeruginosa strains to untreated and oxygen-plasma treated poly (vinyl chloride) (PVC) from endotracheal intubation devices". *Biomaterials* 24.8 (2003): 1507-1518.
86. Park YW and Inagaki N. "Surface modification of poly (vinylidene fluoride) film by remote Ar, H₂, and O₂ plasmas". *Polymer* 44.5 (2003): 1569-1575.
87. J Brutscher, et al. "Sheath dynamics in plasma immersion ion implantation". *Plasma Sources Science and Technology* 5 (1996): 54.
88. AP Kharitonov, et al. "Comparison of the surface modifications of polymers induced by direct fluorination and rf-plasma using fluorinated gases". *Journal of Fluorine Chemistry* 165 (2014): 49-60.
89. I G Broun., et al. "Metal ion implantation: Conventional versus immersion. MacGill". *Journal of Vacuum Science and Technology* B12 (1994): 823.
90. Junkar I., et al. "The role of crystallinity on polymer interaction with oxygen plasma". *Process Polymer* 6 (2009): 667.
91. Wagner P., et al. "Quantitative Assessment to the Structural Basis of Water Repellency in Natural and Technical Surfaces". *Journal of Experimental Botany* 54 (2003): 1295.
92. Okuji S., et al. "Surface modification of polymeric substrates by plasma-based ion implantation". *Nuclear Instruments and Methods in Physics Research Section B: Beam Interactions with Materials and Atoms* 242.1-2 (2006): 353.
93. Marais S., et al. "Effect of a low-pressure plasma treatment on water vapor diffusivity and permeability of poly (ethylene-co-vinyl alcohol) and polyethylene films". *Surface and Coatings Technology* 201.3-4 (2006): 868.
94. Tahara M., et al. "Improvement in adhesion of polyethylene by glow-discharge plasma". *Surface and Coatings Technology* 174-175 (2003): 826.
95. Švorčík V., et al. "Modification of surface properties of high and low density polyethylene by Ar plasma discharge". *Polymer Degradation and Stability* 91.6 (2006): 1219.
96. Jones V., et al. "Development of Poly (propylene) Surface Topography During Corona Treatment". *Plasma Process and Polymer* 2.7 (2005): 547.
97. Karade Y., et al. "Determination of Cross-Link Density in Ion-Irradiated Polystyrene Surfaces from Rippling". *Langmuir* 25.5 (2009): 3108.
98. Karade Y., et al. "Oriented nanometer surface morphologies by thermal relaxation of locally cross-linked and stretched polymer samples". *Microelectronic Engineering* 84.5-8 (2007): 797.
99. Sanchis M R., et al. "Surface modification of low density polyethylene (LDPE) film by low pressure O₂ plasma treatment". *European Polymer Journal* 42.7 (2006): 1558.
100. Mirabedini SM., et al. "Effect of low-pressure O₂ and Ar plasma treatments on the wettability and morphology of biaxial-oriented polypropylene (BOPP) film". *Progress in Organic Coatings* 60.2, (2007): 105.
101. Slepíčka P., et al. "Argon plasma irradiation of polypropylene". *Nuclear Instruments and Methods* 268.11-12 (2010): 2111.
102. Švorčík V., et al. "Modification of surface properties of high and low density polyethylene by Ar plasma discharge". *Polymer Degradation and Stability* 91.6 (2006): 1219.
103. Švorčík V., et al. "Ablation and water etching of poly (ethylene) modified by argon plasma". *Polymer Degradation and Stability* 92.9 (2007): 1645.
104. Reznickova A., et al. "Comparison of glow argon plasma-induced surface changes of thermoplastic polymers". *Nuclear Instruments and Methods in Physics Research Section B: Beam Interactions with Materials and Atoms* 269.2 (2011): 83.
105. Crucho C I., et al. "Surfactant-free polymeric nanoparticles composed of PEG, cholic acid and a sucrose moiety". *Journal of Materials Chemistry B* 2.25 (2014): 3946.
106. Chen J., et al. "Applications of atomic force microscopy in materials, semiconductors, polymers, and medicine: A minireview". *Instrumentation Science and Technology* 48.6 (2020): 667.

107. Lopez R., et al. "Robust Hydrophobic Coatings Using Polymer Blends for the Surface Protection of Marble". *Colloids and Surfaces A: Physicochemical and Engineering Aspects* 599 (2020): 124796.
108. Waranpillai JP., et al. "Intermolecular hydrogen bonding in developing nanostructured epoxy shape memory thermosets: Effects on morphology, thermo-mechanical properties and surface wetting". *Polymer Testing* 81 (2020): 10627.
109. Hasa E., et al. "Manipulation of crosslinking in photo-induced phase separated polymers to control morphology and thermo-mechanical properties". *Polymer* 202 (2020): 122699.
110. Bouali AB., et al. "Nanoscale mechanical properties of chitosan hydrogels as revealed by AFM". *Progress in Biomaterials* 9 (2020): 187.
111. Tamburaci S., et al. "Chitosan-hybrid poss nanocomposites for bone regeneration: The effect of poss nanocage on surface, morphology, structure and *in vitro* bioactivity". *International Journal of Biological Macromolecules* 142 (2020): 643.
112. Hu J and Zhu S. "Microscopy of Shape Memory Polymers, Polymer Blends, and Composites". In: Parameswaranpillai J.; Siengchin S.; George J.; Jose, S. (eds) Shape Memory Polymers, Blends and Composites. *Advanced Structured Materials* 115 (2020): 95.
113. Wu F., et al. "Tailoring the toughness of sustainable polymer blends from biodegradable plastics via morphology transition observed by atomic force microscopy". *Polymer Degradation and Stability* 173 (2020): 109066.
114. Grytsenko K., et al. "Influence of different aligning surfaces on the morphology of dichroic squaraine films". *Polymer Bulletin* 78 (2021): 1313.
115. Nguyen-Tri P., et al. "Recent Applications of Advanced Atomic Force Microscopy in Polymer Science: A Review". *Polymers* 12 (2020): 1142.
116. Sadeghi K and Seo J. "Photografting of p-anisidine-glycidyl methacrylate onto polymeric substrate for developing free-radical scavenging films". *Progress in Organic Coatings* 149 (2020): 105925.
117. Ang M B M Y., et al. "Surface Properties, Free Volume, and Performance for Thin-Film Composite Pervaporation Membranes Fabricated through Interfacial Polymerization Involving Different Organic Solvents". *Polymers* 12.10 (2020): 2326.
118. Chan CM., et al. "Polymer surface modification by plasmas and photons". *Surface Science Reports* 24.1-2 (1996): 1.
119. Grace JM and Gerenser LJ. "Plasma Treatment of Polymers". *Journal of Dispersion Science and Technology* 24 (2003): 341.